

# Irisin may be involved in exendin-4 mitochondrial action in human adipocytes

## Keywords

obesity, irisin, mitochondria, mitochondrial dysfunction, adipocyte, exendin-4, GLP-1RA, browning of WAT

## Abstract

### Introduction

Disturbed mitochondrial activity in adipocytes is suggested as one of the mechanisms involved in metabolic dysfunction in obesity. Glucagon-like peptide receptor agonists (GLP-1RAs) are used to normalize glucose level and reduce body weight. GLP-1 activates similar intracellular pathway as irisin, peptide that modulate metabolism by stimulating the 'browning' of adipocytes. The aim of the study was to investigate the mechanisms of the GLP-1RA, exendin-4, action at the level of mRNA, proteins and mitochondrial activity in human adipocytes.

### Material and methods

The human preadipocytes Chub-S7 were differentiated in vitro to mature adipocytes and then stimulated with exendin-4 at 100 nM for 24 h. Expression of mRNA and proteins (irisin, adiponectin, visfatin/NAMPT) were measured. Oxygen consumption rates and intracellular ATP content were determined.

### Results

The exendin-4 enhanced the secretion of irisin and visfatin by adipocytes. The up-regulated expression of FNDC5, NAMPT and UCP2 genes was accompanied by modest changes in mitochondrial activity in exendin-4 treated adipocytes. Exendin-4 exerted similar effect on mitochondrial oxygen consumption rates as irisin, including increased maximum mitochondrial respiration and reserve capacity with unchanged intracellular ATP.

### Conclusions

Increasing energy expenditure by exendin-4 may be associated with upregulation of irisin in human adipocytes. Clinical studies are necessary to confirm the hypothesis that nutrients, by stimulating the secretion of GLP-1, may influence the expression of irisin and thus modulate the mitochondrial metabolism of adipocytes.

## Introduction

Obesity is a global pandemic, with profound clinical, social and economic consequences [1] It is a complex, metabolic disease resulting from the expansion of adipose tissue, that depends on the interplay between hyperplasia (proliferation and differentiation of adipose precursor cells) and hypertrophy (increase in adipocyte size) [2]. Recent studies indicate that mitochondrial dysfunction caused by excessive nutrient supply that overwhelms the Krebs cycle and the mitochondrial respiratory chain, may be associated with the development of obesity, oxidative stress and inflammation [3,4]. Prevention of the mitochondrial dysfunction is a potential tool to combat obesity.

Among the factors influencing mitochondrial activity and adipocyte metabolism, the adipomyokine, irisin has been clearly associated with an increase in energy expenditure due to its ability to stimulate the browning of white adipose tissue (WAT) [5]. Browning of WAT is a process of trans-differentiation from white to beige adipocytes, involving mitochondrial biogenesis, uncoupling of mitochondrial respiratory chain and switch from energy accumulation to energy dissipation. Thus strategies aimed at promoting WAT browning may have great potential to improve metabolism and treat obesity, due to the ability of brown adipose tissue (BAT) to dissipate energy through thermogenesis [6]. Recent studies have shown that irisin levels, in addition to physical activity, can also be influenced by diet and certain specific drugs (such as metformin, fenofibrate and all-trans retinoic acid) [7]. Irisin shows beneficial effects on energy homeostasis [8], reduces systemic inflammation [9], modulates metabolic processes [10], increases the whole body metabolic rate by inducing glucose transporter 4 (GLUT-4) expression and stimulating glycolysis in adipocytes [11].

Glucagon-like peptide-1 (GLP-1), along with glucose-dependent insulinotropic polypeptide (GIP), are known incretin hormones in humans, released predominantly in the intestine [12]. These hormones are secreted in response to nutrient intake and stimulate insulin secretion from the pancreas [13]. GLP-1 exerts its effects through the GLP-1 receptor (GLP-1R) in multiple tissues, among others the pancreas, kidneys, adipose tissue, brain and smooth muscles [14]. GLP-1, besides the role in glucose homeostasis, reduces appetite, food intake and body weight [15]. Due to the short half-life of native

GLP-1, GLP-1 receptor agonists (GLP-1RAs) have been developed for therapeutic purposes, such as  
exendin-4, introduced for the treatment of type 2 diabetes (T2D) in the mid-2000s.[16]. Over the last  
decade, GLP-1RA has also gained considerable attention as an effective anti-obesity agent [17–19].

Obese patients with type 2 diabetes treated with exenatide have been shown to have significantly  
increased irisin levels, which correlated with improved metabolic profiles [20], thus suggesting a  
possible interaction between irisin and incretin hormones. In addition, both the GLP-1 insulintropic  
effects and irisin levels are defective in T2D, and their exogenous administration is able to improve  
glycemic control [21,22]. Furthermore, some researchers suggest that irisin can be considered an  
incretin hormone because its secretion is influenced by meals and increases insulin secretion in a  
glucose-dependent manner [23]. Thus, both peptides share direct pancreatic effects. Recent studies  
suggested, that albeit through different receptor pathways, irisin and GLP-1 activate the same  
intracellular signaling proteins e.g. PI-3K, AKT, CREB, ERK1/2. [23].

Based on these reports, the aim of the study was to investigate the effect of exendin-4 on  
mitochondrial function in human preadipocytes, as well as on selected adipokines and irisin secretion.  
Additionally, expressions of FNDC5 gene as a precursor of irisin and NAMPT gene as a precursor of  
visfatin, were examined to validate the results of irisin and visfatin protein secretion.

## Materials and methods

### Cell culture

Chub-S7 is an immortalized cell line provided by Nestle Research Center (*Lausanne, Switzerland*).  
These cells, derived from subcutaneous abdominal adipose tissue, preserved their adipogenic capacity  
and can differentiate into mature adipocytes [24]. The Chub-S7 cells (*Nestle Research Center,  
Lausanne, Switzerland*) were cultured in a mixture DMEM/Ham's F12 1:1 (*Sigma*) supplemented with  
10% Fetal bovine serum (*Sigma*). The cells were incubated in a basal medium, which was serum free  
DMEM/F12 medium, supplemented with 17uM D-panthotenic acid (*Sigma*), 33uM d-biotin (*Sigma*),  
5ug/ml transferrin (*Sigma*), 1nM triiodothyronine (*Sigma*), 5ug/ml insulin (*Sigma*), 500ug/ml fetuin

(*Sigma*), 5ng/ml selenium (*Sigma*). The Chub-S7 cells were differentiated into mature adipocytes by adding 1uM dexamethasone (*Sigma*) and 1uM rosiglithazone (*Cayman*). For the first 48 hours of differentiation were additionally added 500 uM IBMX (*Sigma*). The differentiation process lasted 21 days. The differentiated adipocytes were exposed to the following factors: irisin (250ng/ml) or GLP-1R agonist exendin-4 (Ex-4) (100nM) or GLP-1R antagonist exendin-9 (Ex-9) (100nM), for 24 hours.

### **Oil-Red-O staining**

In order to assess the differentiation of cells Chub-S7 adipocytes, lipid droplets in cells were stained with red oil dye. The cells were fixed by use 4% solution paraformaldehyde (*POCH, Gliwice, Poland*) and then, incubated 1 hour with red oil dye (*Sigma*), according to the protocol provided by manufacturer. Next, these cells was visualized under a microscope *Nikon ECLIPSE TS100*.

### **Protein secretion**

Irisin, visfatin/NAMPT and adiponectin levels in the culture medium / cell lysate were measured using enzyme-linked immunosorbent assay (*ELISA*). Irisin levels were measured by Irisin ELISA Kit (limit of quantification [LoQ]—1 ng/mL; *BioVendor-Research and Diagnostic Products, Brno, Czech Republic*). The human visfatin (Nampt) (IntraCellular) ELISA Kit (LoQ—30 pg/mL; *BioVendor-Research and Diagnostic Products, Brno, Czech Republic*) was used to measure visfatin levels. For visfatin determinations, 10x diluted culture medium was used, and for intracellular NAMPT determinations, 1000x diluted cell lysate was used. Results from NAMPT were calculated with Magellan 6 software as pg NAMPT and then adjusted for protein content and reported as pg NAMPT/ $\mu$ g of cell protein. Protein content was measured in the samples of cell lysates by Total Protein Kit, Micro Lowry, Peterson's Modification (*Sigma*). Adiponectin were measured by Human Total Adiponectin/Acrp30 ELISA Kit (LoQ – 0.891 ng/ml; *Bio-Techne,R&D Systems, USA*). All the steps were performed strictly in accordance with the kit instructions.

### **Relative gene expression**

The quantitative expression analysis of *UCP1*, *UCP2* (uncoupling proteins), *NAMPT* (nicotinamide phosphoribosyltransferase) and *FNDC5* (fibronectin type III domain – containing protein 5) as performed by real-time PCR using *18S rRNA (Hs03003631\_g1)* (*Applied Biosystems*) as the reference gene.

Following incubation, total RNA was isolated from cells using TRIzol® Plus RNA Purification System (*Life Technologies, Carlsbad, CA, USA*). The quality of RNA was confirmed by analysis on the NanoDrop (*Thermo Fisher Scientific, Wilmington, DE, USA*). One microgram of total RNA was reverse transcribed using a reverse transcription kit (High Capacity cDNA Reverse Transcription Kit (*Applied Biosystems, Carlsbad, CA, USA*) with random primers. Subsequently, cDNA was subjected to real-time PCR. Quantitative real-time polymerase chain reaction (qPCR) was performed with the TaqMan Gene Expression Assays, according to the manufacturer's protocol using TaqMan primers for *UCP1* (Hs00222453\_m1), *UCP2* (Hs01075227\_m1), *NAMPT* (Hs00237184\_m1), *FNDC5* (Hs00401006\_m1) (*Applied Biosystems, Carlsbad, CA, USA*). Amplification was performed using the continuous fluorescence detection system 7900 HT Fast Real Time PCR system (*Applied Biosystems, Carlsbad, CA, USA*). Data were obtained in a form of sigmoid amplification plots in which fluorescence was plotted against the number of cycles. The threshold cycle (CT) served as a measurement of the starting template amount in each sample. Expression ratio was calculated as normalized CT difference between the control probe and the sample.

### **Oxygen consumption**

Mitochondrial respiration was determined by high-resolution respirometry using an Oxygraph-2k (*O2k; OROBOROS Instruments, Austria, Innsbruck*) according to the phosphorylation control protocol for intact cells [25]. For respirometric analysis cells were cultured in 25cm<sup>2</sup> flasks, trypsinized and counted in the Bürker chamber. Then, the cells suspension were diluted with cultured medium to an appropriate concentration of 10<sup>6</sup> cells/ml and 2ml samples of cells suspension were added to the Oxygraph chambers. The protocol according to Dunham-Snary et al. [26] was used. The following

working concentrations for each mitochondrial effector were selected: 2  $\mu\text{g}/\text{mL}$  oligomycin, 0,5-3,0  $\mu\text{M}$  FCCP (p- trifluoromethoxy carbonyl cyanide phenyl hydrazone), 12  $\mu\text{M}$  antimycin A (AA), and 3  $\mu\text{M}$  rotenone (Rote). Before each experiment, the polarographic oxygen sensors (OroboPOS, POS) were calibrated by a two-point calibration, routinely achieved at air saturation and zero oxygen concentration according to the protocol by [27]. Accordingly, static calibration involved the determination of the constant signal of the POS recorded at 100% and 0% air saturation (achieved with Na-dithionite, OroboPOS-Service Kit) under the particular experimental conditions (temperature, signal amplification by electronic gain, polarization voltage, stirring speed, medium). The procedure used for background correction has been described in detail by Gnaiger E. et al. [28].

The protocol for oxygen consumption rate (OCR) measurement in the intact cells included in sequence: (I) a short period of routine respiration (routine), reflecting the aerobic metabolic activity under cellular routine conditions, (II) oligomycin, which is ATP synthase inhibitor and blocks oxidative phosphorylation and the electron transport chain. (III) FCCP titration, which yields the maximum stimulated respiration, as a measure of electron transport system capacity of uncoupled mitochondria; (IV) antimycin A- inhibitor of mitochondrial respiratory complex III and rotenone - inhibitor of mitochondrial respiratory complex I. Cellular bioenergetic parameters including ATP- and non-ATP- linked oxygen consumption as well as maximal oxygen consumption and reserve capacity were calculated (Figure 1).

### **Intracellular ATP content**

The intracellular ATP content was measured using ATPlite™ Luminescence ATP Detection Assay System (*Perkin Elmer, Waltham, MA, USA*), according to the protocol provided by the manufacturer, and the luminescence was measured using a Tecan Genios micropate reader (*Thermo Fisher*). Results were calculated with Magellan 6 software as nmol ATP and then normalized for protein content in the sample. Protein content was measured in the samples of cell lysates by Total

Protein Kit, Micro Lowry, Peterson's Modification (*Sigma*). Finally, results were reported as nmol ATP/mg of cell protein.

### Statistical analysis

All data were expressed as the mean  $\pm$ S.D. from three independent experiments (biological replicates) measured in technical triplicates. Statistical significance for comparisons between treated and control cell samples were determined by the unpaired t-test using Statistica 10.0 PL software.

## Results

### Cell differentiation

The changes in morphology of Chub-S7 cells and lipid droplets accumulation were observed with the light microscopy. After 21 days of differentiation process, the cells were stained with Oil Red-O. The lipid droplets in the cells turned red (Figure 2), which confirmed that preadipocytes differentiated into mature, functional adipocytes, used for further research.

### Protein secretion

Analysis of proteins secretion indicated that Chub-S7 cells exposed to Ex-4 released significantly more irisin (Figure 3. A) and visfatin (Figure 3. C) to cell culture supernatant as well as presented higher intracellular NAMPT level than control cells (Figure 3. D). In case of adiponectin no significant changes were observed in Chub-S7 cells incubated with Ex-4 (Figure 3. B). To confirm the specificity of effects exerted by Ex-4 in Chub-S7 cells, the experiments were repeated using 100 nM exendin-9, the antagonist of GLP-1 receptor, that reverted the effects of Ex-4 on protein secretion.

### Gene expression

Selected genes were examined: (i) genes related to mitochondrial uncoupling (*UCP1*, *UCP2*), (ii) gene encodes transmembrane protein fibronectin type III domain – containing protein 5 precursor of irisin (*FNDC5*) and (iii) gene related to NAD<sup>+</sup> synthesis (*NAMPT*) (Figure 4). The expression of *UCP*

genes is related to discharge of the proton gradient that is generated by the mitochondrial respiratory chain. The *UCP2* gene was up-regulated in Chub-S7 cells incubated with Ex-4, while the expression of the *UCP1* gene only tended to be slightly increased in Ex-4 treated cells. Ex-4 increased more than threefold the expression of *FNDC5* gene coding for irisin and *NAMPT*, coding for a key nicotinamide adenine dinucleotide (NAD) biosynthetic enzyme in mammals. Exendin-9 abolished these effects of GLP-1receptor agonist thus confirmed that they were related to Ex-4.

### Oxygen consumption

Mitochondrial respiration was analyzed by high-resolution respirometry using Oxygraph-2k.

Exploratory observations of oxygen consumption revealed differences between cells treated with the irisin or Ex-4 and control cells. The addition of exendin-9 together with Ex-4 abolished the effect of GLP-1RA (Table I).

Basal OCR was slightly increased in irisin treated cells (Figure 5 A). When the non-mitochondrial oxygen consumption, measured after full inhibition of mitochondrial electron transport chain by antimycin A and rotenone, was subtracted, the routine mitochondrial respiration was increased in the irisin and Ex-4 treated cells. ATP-linked oxygen consumption, calculated as the difference between basal oxygen consumption and OCR measured after the addition of oligomycin to inhibit complex V, remained similar regardless the exposition of adipocytes. In contrast, the non-ATP- linked oxygen consumption, tended to increase in cells exposed to irisin or Ex-4 compared to controls (Figure 5 B). Further analysis of mitochondrial respiratory states revealed the significantly increased maximal mitochondrial OCR both in irisin and in Ex-4 treated cells after stimulation of the uncoupling of electron transport chain from ATP synthesis in mitochondria by FCCP. Reserve capacity, calculated by subtracting the basal OCR from the maximal oxygen consumption after the addition of FCCP, was found to slightly increase in similar way after incubation with irisin or Ex-4 (Figure 5 C). Addition of exendin-9 to GLP-1RA caused OCR to be restored to control values showing that the observed

changes in mitochondrial oxygen consumption rates were dependent on Ex-4/ GLP-1R interaction (Figure 5).

### **Intracellular ATP content**

No changes in intracellular ATP content were observed in Chub-S7 cells exposed to irisin or Ex-4 (Figure 6). These results show that in the presented experiment, the increased mitochondrial oxygen consumption rate was not associated with raised ATP synthesis.

### **Discussion**

Our previous work has shown that Ex-4 may affect the mitochondrial bioenergetics in human adipocytes by enhanced expression of sirtuins (1 and 3) [29]. Based on these results, in the current study, we investigated also the effect of GLP-1RA on selected adipokines secretion (irisin, visfatin/NAMPT and adiponectin), related to sirtuins pathway. It has been reported that adiponectin prevents mitochondrial dysfunction in a sirtuin-3 (SIRT3) dependent manner [30]. Furthermore, SIRT3 is an NAD(+)-dependent deacetylase which functions in conjunction with mitochondrial NAMPT to promote cell survival following genotoxic stress [31].

Simental-Mendía et al. in a meta-analysis of randomized controlled trials reported an increase in adiponectin concentrations in the course of GLP-1RA therapy [32]. They demonstrated a significant increase in serum adiponectin levels after liraglutide, while exenatide had no effect, which is consistent with our results. In our in vitro study, no significant changes in adiponectin secretion to the cell culture supernatant after incubation of Chub-S7 cells with Ex-4 were observed. The opposite results were obtained by Chung et al. [33] who showed that Ex-4 upregulated adiponectin synthesis in 3T3-L1 adipocytes through PKA expression and/or PKA activity. In our study, although adiponectin remain unchanged under Ex-4, secretion of another adipokine –irisin was significantly increased. This finding is in line with the paper by Liu et al. [20] demonstrated that exenatide significantly increased

serum irisin levels in patients with T2D. These results suggest that the upregulation of irisin might be a novel mechanism for the beneficial effects of exenatide in patients with T2D.

Visfatin is one of the adipocytokines, with insulin mimetic activity, which enzymatic function is the same as NAMPT [34]. Our results showed that Ex-4 increased visfatin secretion to the culture medium and intracellular NAMPT level. A similar effect on visfatin was observed in other studies that showed that GLP-1 induced secretion of visfatin into the culture medium of 3T3-L1 adipocytes due to increased visfatin mRNA expression [35].

Data from presented study showed that Ex-4 significantly upregulated not only protein but also *NAMPT* gene expression. Similar results were obtained by Lee et al. [36] in the experiment on C57BL/6J mice, showing that *NAMPT* expression was induced by Ex-4 treatment. Furthermore, the data suggests that Ex-4 treatment may increase sirtuins expression via the NAD<sup>+</sup> biosynthesis pathway. Indeed, our previous work has shown that Ex-4 significantly increases expression of *SIRT1* [29]. Recent studies have demonstrated that NAMPT deficiency induces adipose tissue dysfunction and insulin resistance, and altered whole-body energy and glucose metabolism [37,38]. These findings suggest that Ex-4 may have a beneficial effect on metabolic abnormalities by influencing postprandial glycemia also through an increase in the expression of the *NAMPT* gene. Furthermore, NAMPT-mediated NAD<sup>+</sup> biosynthesis and sirtuins in the intestine, are critical for intestinal homeostasis, including GLP-1 production [39].

Our data showed that Ex-4 up-regulated the expression of *UCP2*, responsible together with *UCP1* for heat generation and non-shivering thermogenesis in brown adipose tissue. In the presence of UCPs, a high respiratory rate occurs in the absence of ATP production. Uncoupling protein 2 plays a role in fatty acid and glucose metabolism and transportation of TCA cycle metabolites. The role of uncoupling proteins in various metabolic conditions, like diabetes or obesity, has been reported [40].

Recent studies have demonstrated that *FNDC5* expression and secretion of irisin from adipocytes, is lower in patients with obesity and T2D than in lean controls [41]. In our study, Ex-4 upregulated the expression of the *FNDC5* gene. This is of more importance as irisin is known to suppresses oxidative

stress by retaining mitochondrial biogenesis and dynamics and exerts a protective effect by promoting 227  
SIRT3-dependent mitochondrial quality control [42,43]. In addition, it has been shown, that irisin 228  
treatment targets uncoupling protein 2 (UCP2) and activates the AMPK-Nrf2 pathway, substantially 229  
improving oxidative stress and mitochondrial dysfunction [44]. 230

We also examined the influence of Ex-4 and irisin on mitochondrial functions in human 231  
adipocytes to compare the effects of these peptides. Our results showed that both irisin and Ex-4 232  
increased maximum OCR. Recently, another study has presented the similar effect of irisin on the 233  
metabolic function of osteoclast progenitors during differentiation, where treatment with 10 ng/mL of 234  
irisin for 48 h significantly increased maximal respiration, associated with increased mitochondrial 235  
content showed by fluorescent imaging [45]. In parallel, Jansen et al. [46] showed that the GLP-1 236  
analogue exenatide increases hepatic mitochondrial respiration in high-fat fed mice in the various 237  
respiratory states, such as LEAK, OXPHOS and ETS. In our study, both irisin and Ex-4 independently 238  
increased also non-ATP linked OCR, while intracellular ATP content remain unchanged. This 239  
confirms our earlier report that increased mitochondrial OCR was accompanied by slightly decreased 240  
mitochondrial membrane potential but not excessive ATP synthesis in mature adipocytes exposed to 241  
Ex-4 [29]. Such subtle effects may reflect functional adaptations of mitochondria to conditions that 242  
require ATP generation or energy dissipation. Nutrients excess or physical activity, are sensed at the 243  
organismal and cellular levels, activating hormonal, metabolite or protein signalling that control 244  
mitochondrial-linked gene transcription and mRNA translation to enhance respiratory capacity [47]. 245  
Thus mild effects of both the nutrient sensitive peptides: GLP-1RA, exendin-4, and irisin on 246  
mitochondrial respiration observed in our study, may be a part of an adaptive response, preventing 247  
mitochondrial damage and subsequent proinflammatory and dysfunctional adipocytes. 248

To summarize, results from our study showed that Ex-4 influences the expression of genes related 249  
to mitochondrial biogenesis, energy expenditure and mitochondrial uncoupling, including *FNDC5* 250  
coding for irisin as well as mildly stimulates the mitochondrial activity. The finding that changes in 251  
mRNA and respective proteins expression are further reflected in mitochondrial bioenergetics is a 252

strength of the study, as is the unique cell model. However, due to the limited data collected on 253  
mitochondrial metabolism, the results presented here should be considered as preliminary, providing a 254  
basis for further studies in animal models and clinical samples, supporting the hypothesis that irisin 255  
may mediate the action of GLP-1RAs. In order to understand in detail the action of irisin and confirm 256  
whether it mediates exendin-4 effects, it would also be interesting to perform experiments with 257  
simultaneous silencing of the FNDC5 gene. 258

Although the study has yielded interesting results, it has some limitations. One of the 259  
shortcomings is that the *in vitro* Chub-S7 model derived from preadipocytes of a single obese 260  
individual does not reflect biological variability. It would be worthwhile to repeat the study on 261  
adipocytes from different donors, but this is difficult due to invasiveness and ethical considerations. 262  
On the other hand, such a model allows the detection of even mild effects due to the high repeatability 263  
of the results. Indeed, the fold change of selected genes expression is not impressive, thus may reduce 264  
the strength of our observations. In our study, the observed effect of Ex-4 on mitochondrial activity 265  
was also rather mild. These modest effects may be due to the low level of GLP-1R expression in 266  
adipose tissue. Some authors have hypothesized that in humans, GLP-1R expression is more abundant 267  
in visceral adipose tissue (VAT), especially in obese subjects with a high insulin-resistant profile [48]. 268  
Although the expression of GLP-1R is well documented in human preadipocytes and adipocytes [48], 269  
the level of expression may be different in various types of adipocytes, thus it would be interesting to 270  
investigate the expression of GLP-1R at the mRNA or protein level in our cell model. In our research, 271  
we used the subcutaneous adipose tissue cell model (Chub-S7 cells) due to the small number of 272  
publications in this field. Further additional studies should be conducted with higher statistical power 273  
to confirm the observed associations. 274

In conclusion, stimulation of human adipocytes *in vitro* by GLP-1RA, Ex-4, enhance the 275  
expression of irisin on the mRNA and protein levels. Ex-4 and irisin similarly increase energy 276  
expenditure in human adipocytes, the mechanism of action that is beneficial in the treatment of 277  
obesity. Given the limitations of the *in vitro* model using one human adipocyte cell line, further studies 278

are necessary to confirm the hypothesis that nutrients, by stimulating the secretion of GLP-1, may 279  
influence the expression of irisin and thus modulate the mitochondrial metabolism of adipocytes. 280

281

**Conflicts of Interest:** The authors declare no conflicts of interest. 282

283

Preprint

## REFERENCES

1. Brauer, M.; Roth, G.A.; Aravkin, A.Y.; Zheng, P.; Abate, K.H.; Abate, Y.H.; Abbafati, C.; Abbasgholizadeh, R.; Abbasi, M.A.; Abbasian, M.; et al. Global Burden and Strength of Evidence for 88 Risk Factors in 204 Countries and 811 Subnational Locations, 1990–2021: A Systematic Analysis for the Global Burden of Disease Study 2021. *The Lancet* **2024**, *403*, 2162–2203, doi:10.1016/S0140-6736(24)00933-4.
2. Horwitz, A.; Birk, R. Adipose Tissue Hyperplasia and Hypertrophy in Common and Syndromic Obesity – The Case of BBS Obesity. *Nutrients* **2023**, *15*.
3. de Mello, A.H.; Costa, A.B.; Engel, J.D.G.; Rezin, G.T. Mitochondrial Dysfunction in Obesity. *Life Sci* **2018**, *192*, 26–32.
4. Patti, M.E.; Corvera, S. The Role of Mitochondria in the Pathogenesis of Type 2 Diabetes. *Endocr Rev* **2010**, *31*, 364–395.
5. Liu, S.; Cui, F.; Ning, K.; Wang, Z.; Fu, P.; Wang, D.; Xu, H. Role of Irisin in Physiology and Pathology. *Front Endocrinol (Lausanne)* **2022**, *13*.
6. Al-Amrani, A.; AbdelKarim, M.; AlZabin, M.; Alzoghaibi, M. Low Expression of Brown and Beige Fat Genes in Subcutaneous Tissues in Obese Patients. *Archives of Medical Science* **2019**, *15*, 1113–1122, doi:10.5114/aoms.2018.76684.
7. Flori, L.; Testai, L.; Calderone, V. The “Irisin System”: From Biological Roles to Pharmacological and Nutraceutical Perspectives. *Life Sci* **2021**, *267*.
8. Korta, P.; Pocheć, E.; Mazur-Biały, A. Irisin as a Multifunctional Protein: Implications for Health and Certain Diseases. *Medicina (Lithuania)* **2019**, *55*.
9. Slate-Romano, J.J.; Yano, N.; Zhao, T.C. Irisin Reduces Inflammatory Signaling Pathways in Inflammation-Mediated Metabolic Syndrome. *Mol Cell Endocrinol* **2022**, *552*.
10. Bao, J.F.; She, Q.Y.; Hu, P.P.; Jia, N.; Li, A. Irisin, a Fascinating Field in Our Times. *Trends in Endocrinology and Metabolism* **2022**, *33*, 601–613.
11. Huh, J.Y.; Dincer, F.; Mesfum, E.; Mantzoros, C.S. Irisin Stimulates Muscle Growth-Related Genes and Regulates Adipocyte Differentiation and Metabolism in Humans. *Int J Obes* **2014**, *38*, 1538–1544, doi:10.1038/ijo.2014.42.
12. Wu, T.; Rayner, C.K.; Horowitz, M. Incretins. *Handb Exp Pharmacol* **2015**, *233*, 137–171, doi:10.1007/164\_2015\_9.
13. Nauck, M.A.; Meier, J.J. Incretin Hormones: Their Role in Health and Disease. *Diabetes Obes Metab* **2018**, *20*, 5–21.
14. Chia, C.W.; Egan, J.M. Incretins in Obesity and Diabetes. *Ann N Y Acad Sci* **2020**, *1461*, 104–126.
15. Nauck, M.A.; Quast, D.R.; Wefers, J.; Pfeiffer, A.F.H. The Evolving Story of Incretins (GIP and GLP-1) in Metabolic and Cardiovascular Disease: A Pathophysiological Update. *Diabetes Obes Metab* **2021**, *23*, 5–29.
16. Garber, A.J. Novel GLP-1 Receptor Agonists for Diabetes. *Expert Opin Investig Drugs* **2012**, *21*, 45–57.
17. Lorza-Gil, E.; Strauss, O.D.; Ziegler, E.; Kansy, K.; Katschke, M.T.; Rahimi, G.; Neuscheler, D.; Sandforth, L.; Sandforth, A.; Sancar, G.; et al. Incretin-Responsive Human Pancreatic Adipose Tissue Organoids: A Functional Model for Fatty Pancreas Research. *Mol Metab* **2025**, *91*, doi:10.1016/j.molmet.2024.102067.
18. Zhao, Q.; Yang, Y.; Hu, J.; Shan, Z.; Wu, Y.; Lei, L. Exendin-4 Enhances Expression of Neurod1 and Glut2 in Insulin-Producing Cells Derived from Mouse Embryonic Stem Cells. *Archives of Medical Science* **2016**, *12*, 199–207, doi:10.5114/aoms.2016.57596.
19. Alhomoud, I.S.; Talasaz, A.H.; Chandrasekaran, P.; Brown, R.; Mehta, A.; Dixon, D.L. Incretin Hormone Agonists: Current and Emerging Pharmacotherapy for Obesity Management. *Pharmacotherapy* **2024**, *44*.

20. Liu, J.; Hu, Y.; Zhang, H.; Xu, Y.; Wang, G. Exenatide Treatment Increases Serum Irisin Levels in Patients with Obesity and Newly Diagnosed Type 2 Diabetes. *J Diabetes Complications* **2016**, *30*, 1555–1559, doi:10.1016/j.jdiacomp.2016.07.020. 325–327
21. Nauck, M.A.; Meier, J.J. The Incretin Effect in Healthy Individuals and Those with Type 2 Diabetes: Physiology, Pathophysiology, and Response to Therapeutic Interventions. *Lancet Diabetes Endocrinol* **2016**, *4*, 525–536. 328–329
22. Perakakis, N.; Triantafyllou, G.A.; Fernández-Real, J.M.; Huh, J.Y.; Park, K.H.; Seufert, J.; Mantzoros, C.S. Physiology and Role of Irisin in Glucose Homeostasis. *Nat Rev Endocrinol* **2017**, *13*, 324–337. 330–331
23. Marrano, N.; Biondi, G.; Borrelli, A.; Cignarelli, A.; Perrini, S.; Laviola, L.; Giorgino, F.; Natalicchio, A. Irisin and Incretin Hormones: Similarities, Differences, and Implications in Type 2 Diabetes and Obesity. *Biomolecules* **2021**, *11*, 1–23. 332–334
24. Darimont, C.; Zbinden, I.; Avanti, O.; Leone-Vautravers, P.; Giusti, V.; Burckhardt, P.; Pfeifer, A.M.A.; Macé, K. Reconstitution of Telomerase Activity Combined with HPV-E7 Expression Allow Human Preadipocytes to Preserve Their Differentiation Capacity after Immortalization. *Cell Death Differ* **2003**, *10*, 1025–1031, doi:10.1038/sj.cdd.4401273. 335–338
25. Gnaiger, E.; Renner-Sattler, K. *Phosphorylation Control Protocol with Intact Cells: ROUTINE, LEAK, ETS, ROX*; 2011; 339
26. Dunham-Snary, K.J.; Sandel, M.W.; Westbrook, D.G.; Ballinger, S.W. A Method for Assessing Mitochondrial Bioenergetics in Whole White Adipose Tissues. *Redox Biol* **2014**, *2*, 656–660, doi:10.1016/j.redox.2014.04.005. 340–341
27. Gnaiger E *Oroboros O2k-FluoRespirometer High-Resolution Respirometry O2k-Calibration by DatLab*; 2016; Vol. 19;. 342
28. Gnaiger, E. Bioenergetics at Low Oxygen: Dependence of Respiration and Phosphorylation on Oxygen and Adenosine Diphosphate Supply. In *Proceedings of the Respiration Physiology; Respir Physiol*, 2001; Vol. 128, pp. 277–297. 343–345
29. Góralaska, J.; Śliwa, A.; Gruca, A.; Rażny, U.; Chojnacka, M.; Polus, A.; Solnica, B.; Malczewska-Malec, M. Glucagon-like Peptide-1 Receptor Agonist Stimulates Mitochondrial Bioenergetics in Human Adipocytes. *Acta Biochim Pol* **2017**, *64*, 423–429, doi:10.18388/abp.2017\_1634. 346–348
30. Zhang, S.; Wu, X.; Wang, J.; Shi, Y.; Hu, Q.; Cui, W.; Bai, H.; Zhou, J.; Du, Y.; Han, L.; et al. Adiponectin/AdiopR1 Signaling Prevents Mitochondrial Dysfunction and Oxidative Injury after Traumatic Brain Injury in a SIRT3 Dependent Manner. *Redox Biol* **2022**, *54*, doi:10.1016/j.redox.2022.102390. 349–351
31. Shackelford Rodney; Hirsh Sharon; Henry Katherine; Abdel-Mageed Asim; Kandil Emad; Coppola Domenico Nicotinamide Phosphoribosyltransferase and SIRT3 Expression Are Increased in Well-Differentiated Thyroid Carcinomas | *Anticancer Research* (accessed on 15 January 2025). 352–354
32. Simental-Mendía, L.E.; Sánchez-García, A.; Linden-Torres, E.; Simental-Mendía, M. Impact of Glucagon-like Peptide-1 Receptor Agonists on Adiponectin Concentrations: A Meta-Analysis of Randomized Controlled Trials. *Br J Clin Pharmacol* **2021**, *87*, 4140–4149. 355–357
33. Kim Chung, L.T.; Hosaka, T.; Yoshida, M.; Harada, N.; Sakaue, H.; Sakai, T.; Nakaya, Y. Exendin-4, a GLP-1 Receptor Agonist, Directly Induces Adiponectin Expression through Protein Kinase A Pathway and Prevents Inflammatory Adipokine Expression. *Biochem Biophys Res Commun* **2009**, *390*, 613–618, doi:10.1016/j.bbrc.2009.10.015. 358–361
34. Sommer, G.; Garten, A.; Petzold, S.; Beck-Sickinger, A.G.; Blüher, M.; Stumvoll, M.; Fasshauer, M. Visfatin/PBEF/Nampt: Structure, Regulation and Potential Function of a Novel Adipokine. *Clin Sci* **2008**, *115*, 13–23. 362–364
35. Liu, R.; Ding, X.; Wang, Y.; Wang, M.; Peng, Y. Glucagon-like Peptide-1 Upregulates Visfatin Expression in 3T3-L1 Adipocytes. *Hormone and Metabolic Research* **2013**, *45*, 646–651, doi:10.1055/s-0033-1343472. 365–366

36. Lee, J.; Hong, S.W.; Chae, S.W.; Kim, D.H.; Choi, J.H.; Bae, J.C.; Park, S.E.; Rhee, E.J.; Park, C.Y.; Oh, K.W.; et al. Exendin-4 Improves Steatohepatitis by Increasing Sirt1 Expression in High-Fat Diet-Induced Obese C57BL/6J Mice. *PLoS One* **2012**, *7*, doi:10.1371/journal.pone.0031394. 367  
368  
369
37. Yamaguchi, S.; Yoshino, J. Adipose Tissue NAD<sup>+</sup> Biology in Obesity and Insulin Resistance: From Mechanism to Therapy. *BioEssays* **2017**, *39*. 370  
371
38. Stromsdorfer, K.L.; Yamaguchi, S.; Yoon, M.J.; Moseley, A.C.; Franczyk, M.P.; Kelly, S.C.; Qi, N.; Imai, S. ichiro; Yoshino, J. NAMPT-Mediated NAD<sup>+</sup> Biosynthesis in Adipocytes Regulates Adipose Tissue Function and Multi-Organ Insulin Sensitivity in Mice. *Cell Rep* **2016**, *16*, 1851–1860, doi:10.1016/j.celrep.2016.07.027. 372  
373  
374
39. Nagahisa, T.; Kosugi, S.; Yamaguchi, S. Interactions between Intestinal Homeostasis and NAD<sup>+</sup> Biology in Regulating Incretin Production and Postprandial Glucose Metabolism. *Nutrients* **2023**, *15*. 375  
376
40. Sreedhar, A.; Zhao, Y. Uncoupling Protein 2 and Metabolic Diseases. *Mitochondrion* **2017**, *34*, 135–140. 377
41. Moreno-Navarrete, J.M.; Ortega, F.; Serrano, M.; Guerra, E.; Pardo, G.; Tinahones, F.; Ricart, W.; Fernández-Real, J.M. Irisin Is Expressed and Produced by Human Muscle and Adipose Tissue in Association with Obesity and Insulin Resistance. *Journal of Clinical Endocrinology and Metabolism* **2013**, *98*, doi:10.1210/jc.2012-2749. 378  
379  
380
42. Ge, Y.; Wu, X.; Cai, Y.; Hu, Q.; Wang, J.; Zhang, S.; Zhao, B.; Cui, W.; Wu, Y.; Wang, Q.; et al. FNDC5 Prevents Oxidative Stress and Neuronal Apoptosis after Traumatic Brain Injury through SIRT3-Dependent Regulation of Mitochondrial Quality Control. *Cell Death Dis* **2024**, *15*, doi:10.1038/s41419-024-06748-w. 381  
382  
383
43. Maak, S.; Norheim, F.; Drevon, C.A.; Erickson, H.P. Progress and Challenges in the Biology of FNDC5 and Irisin. *Endocr Rev* **2021**, *42*, 436–456. 384  
385
44. Wen, P.; Sun, Z.; Yang, D.; Li, J.; Li, Z.; Zhao, M.; Wang, D.D.; Gou, F.; Wang, J.; Dai, Y.; et al. Irisin Regulates Oxidative Stress and Mitochondrial Dysfunction through the UCP2-AMPK Pathway in Prion Diseases. *Cell Death Dis* **2025**, *16*, doi:10.1038/s41419-025-07390-w. 386  
387  
388
45. Estell, E.; Ichikawa, T.; Giffault, P.; Bonewald, L.; Spiegelman, B.; Rosen, C. Irisin Enhances Mitochondrial Function in Osteoclast Progenitors during Differentiation. *Biomedicines* **2023**, *11*, doi:10.3390/biomedicines11123311. 389  
390  
391
46. Jansen, K.M.; Dahdah, N.; Gama-Perez, P.; Schots, P.C.; Larsen, T.S.; Garcia-Roves, P.M. Impact of GLP-1 Receptor Agonist versus Omega-3 Fatty Acids Supplement on Obesity-Induced Alterations of Mitochondrial Respiration. *Front Endocrinol (Lausanne)* **2023**, *14*, doi:10.3389/fendo.2023.1098391. 392  
393  
394
47. Bennett, C.F.; Latorre-Muro, P.; Puigserver, P. Mechanisms of Mitochondrial Respiratory Adaptation. *Nat Rev Mol Cell Biol* **2022**, *23*, 817–835. 395  
396
48. Ejarque, M.; Guerrero-Pérez, F.; de la Morena, N.; Casajoana, A.; Virgili, N.; López-Urdiales, R.; Maymó-Masip, E.; Pujol Gebelli, J.; Garcia Ruiz de Gordejuela, A.; Perez-Maraver, M.; et al. Role of Adipose Tissue GLP-1R Expression in Metabolic Improvement after Bariatric Surgery in Patients with Type 2 Diabetes. *Sci Rep* **2019**, *9*, doi:10.1038/s41598-019-42770-1. 397  
398  
399  
400  
401  
402

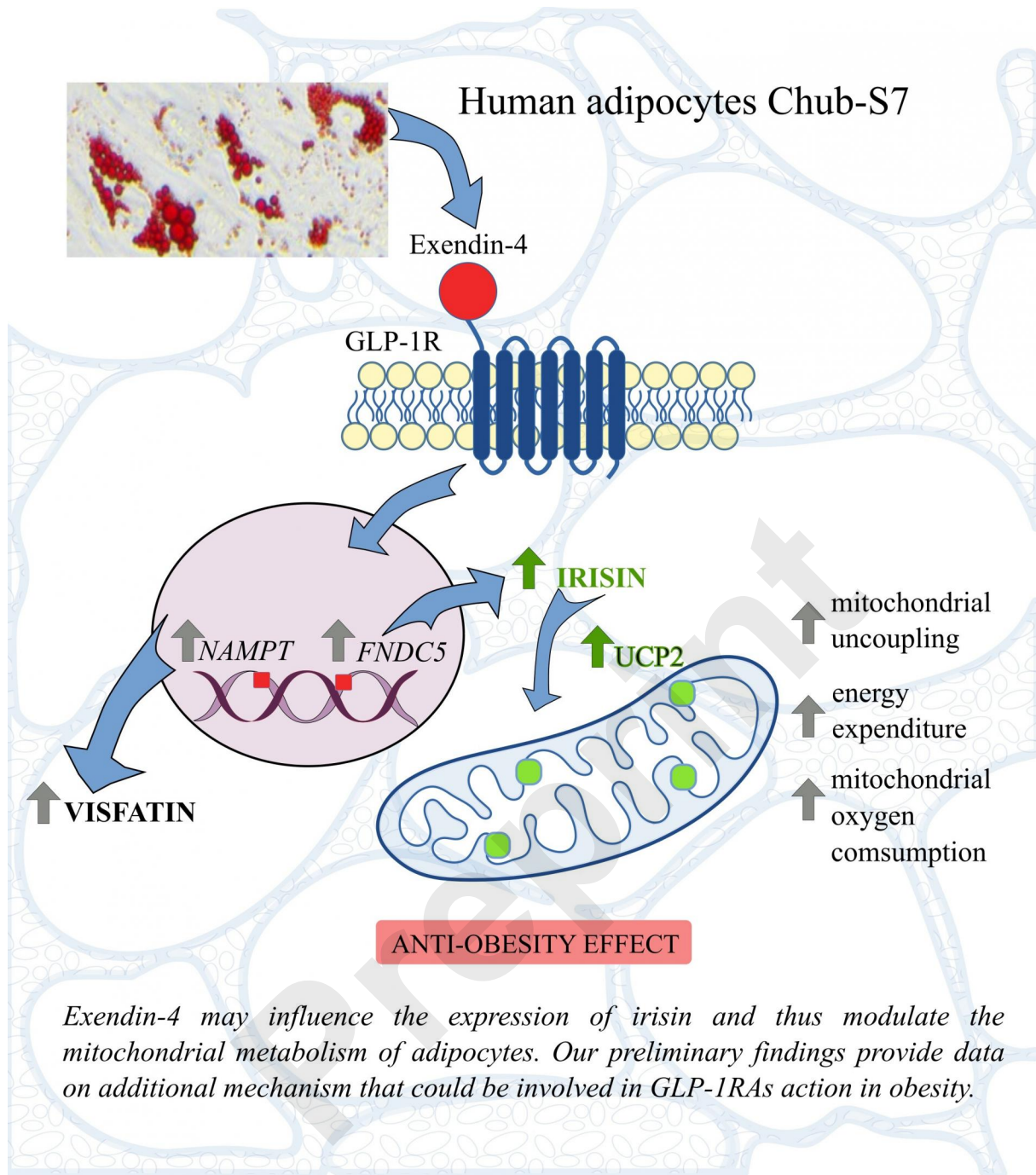


**Table I.** Oxygen consumption rates (OCR) measured by high resolution respirometry in Chub-S7 cells.

	<b>Control</b>	<b>Irisin</b>	<b>Ex-4</b>	<b>Ex-4 + Ex-9</b>
Basal OCR	24.80±2.25	30.67±5.51	29.08±9.28	26.08±4.64
Routine mitochondrial	18.60±1.99	25.67±4.16	24.58±5.30	19.70±0.64
Maximum	47.47±8.83	65.00±6.08	62.81±7.83	52.80±15.35
Non-mitochondrial	6.20±3.34	4.17±3.55	4.50±4.36	6.37±5.07
Maximum mitochondrial	41.27±6.07	59.67±4.16	58.31±3.77	41.76±6.19
Non-ATP-linked	7.75±9.15	11.67±2.52	11.72±3.96	6.61±2.54
ATP-linked	10.84±7.82	11.33±4.04	11.86±5.01	10.18±7.33
Reserve capacity	22.68±6.61	34.33±2.08	33.73±1.54	24.21±8.10

Data represent mean ± standard deviation. All values in pmol/min. *Abbreviations:* Ex-4 - exendin-4; Ex-4 + Ex-9 – exendin-4+exendin-9.

## Oxygen consumption

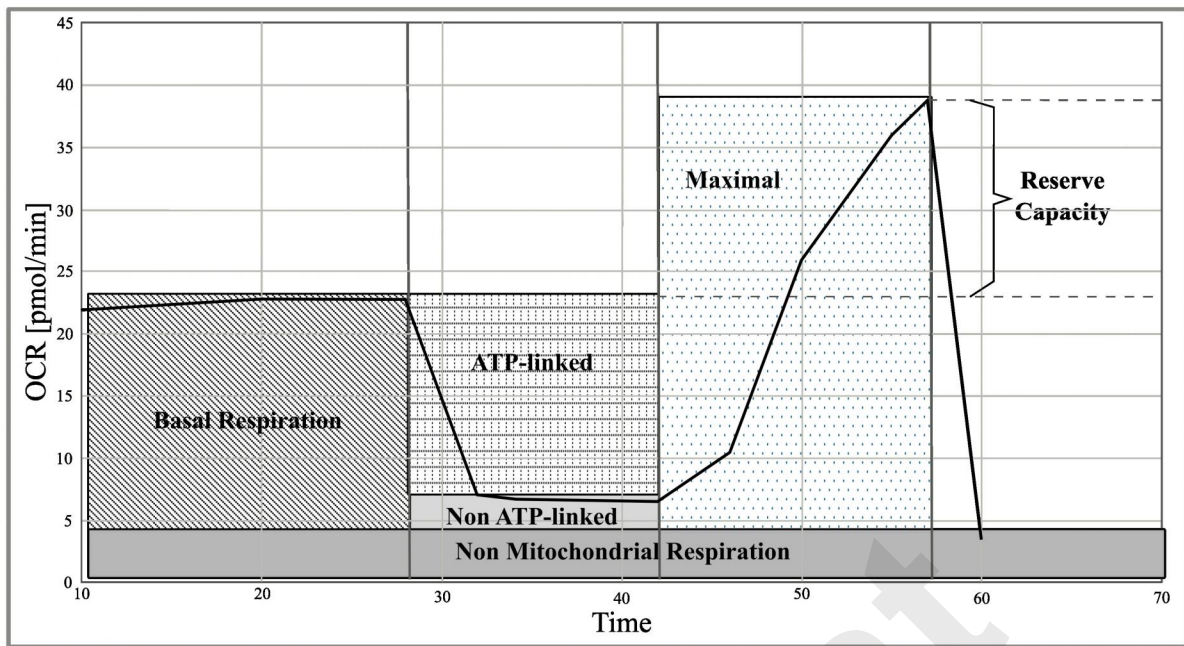
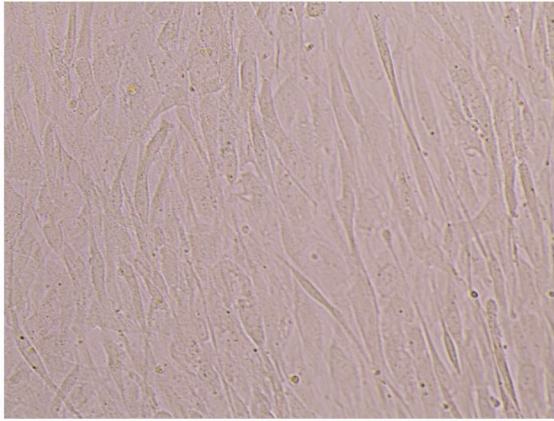
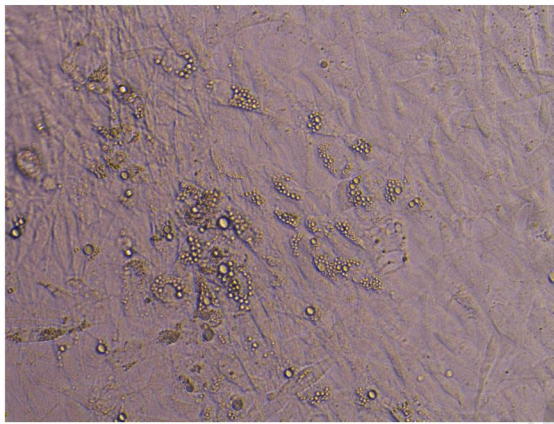


Figure 1. An example trace from oxygen consumption rate (OCR) of Chub-S7 cells. Bioenergetic parameters including basal, ATP-linked and non ATP-linked, maximal oxygen consumption, reserve capacity and non-mitochondrial respiration.

A



B



C

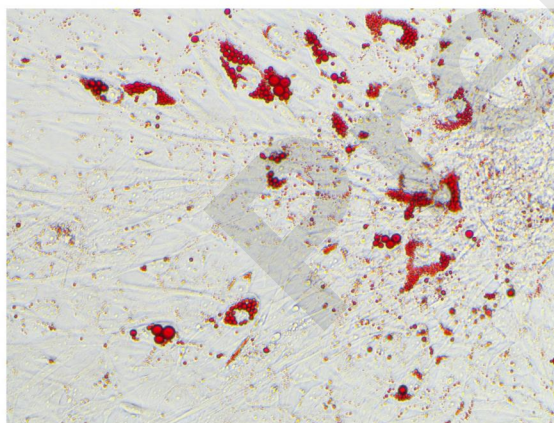


Figure 2. Cell model: (A) Chub-S7 cells prior differentiation; (B) Chub-S7 cells after 21 days of differentiation into mature adipocytes; (C) Chub-S7 after 21 days of differentiation with lipid droplets stained by Oil Red-O ; magnification 200x.

## Protein secretion

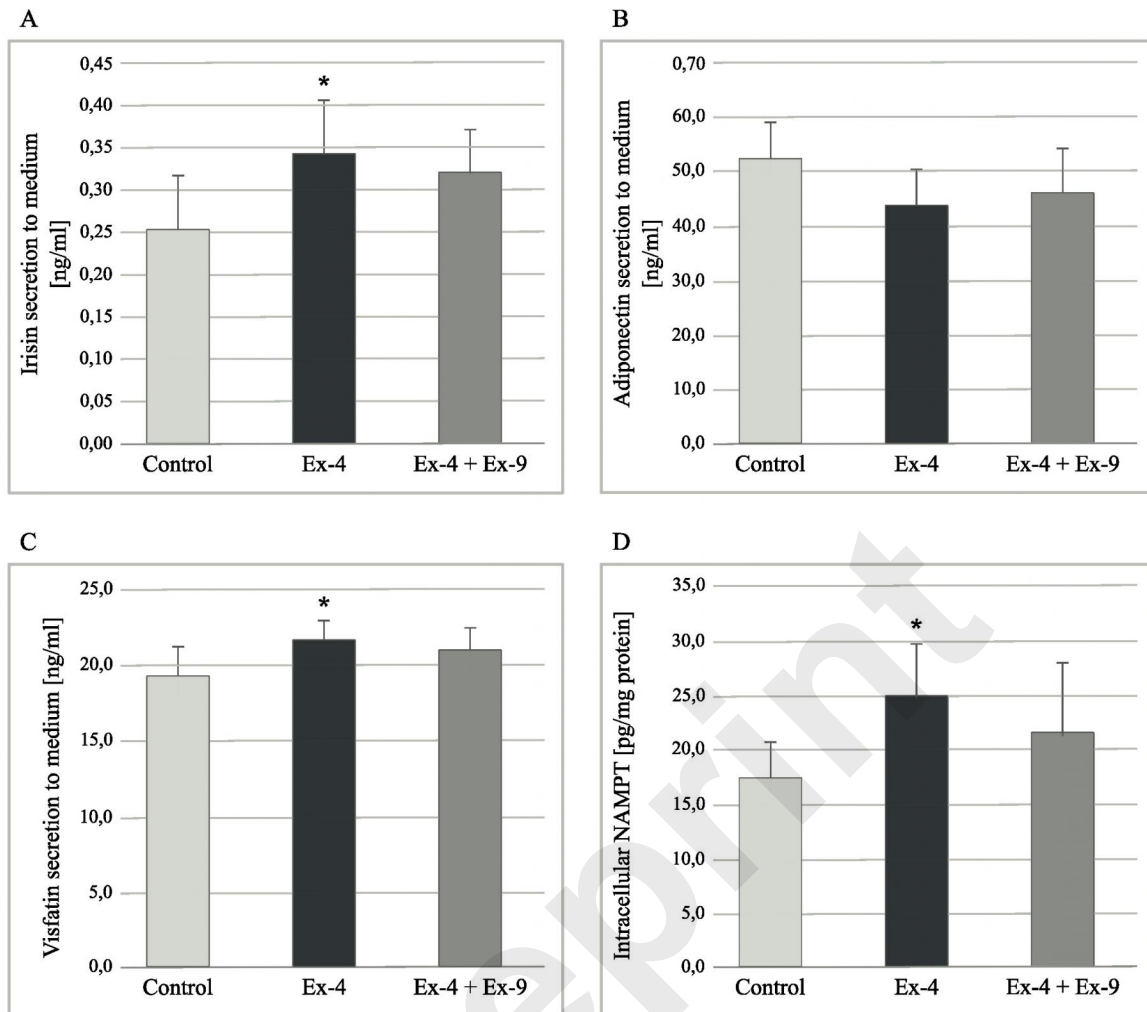


Figure 3. (A) Irisin, (B) adiponectin, (C) visfatin, (D) NAMPT were measured by enzyme-linked immunosorbent assay (ELISA) in cell culture supernatant (A, B, C) or cell lysate (D) after exposure for exendin-4 (Ex-4) (100 nM, 24 h) or exendin-4 (100 nM, 24 h) along with exendin-9 (100 nM, 24 h) (Ex-4 + Ex-9). Values are mean +S.D (n=3) analysed by T-test, \*p<0.05 compared to control.

## Gene expression

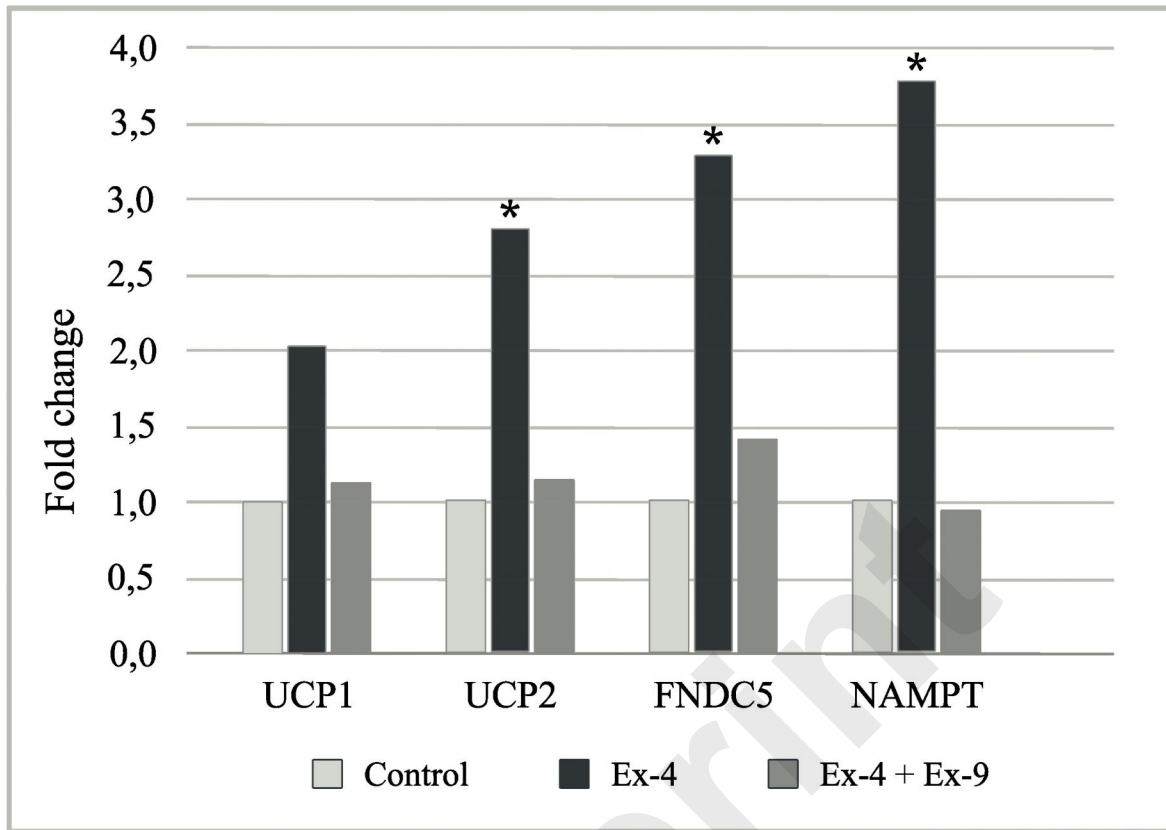


Figure 4. Changes in relative gene expression of selected genes: UCP1, UCP2, FNDC5 and NAMPT. As a reference gene, expression of 18Sr-RNA was used. Values are mean +S.D (n=3) analysed by T-test, \*p<0,05 compared to control.

## Oxygen consumptions

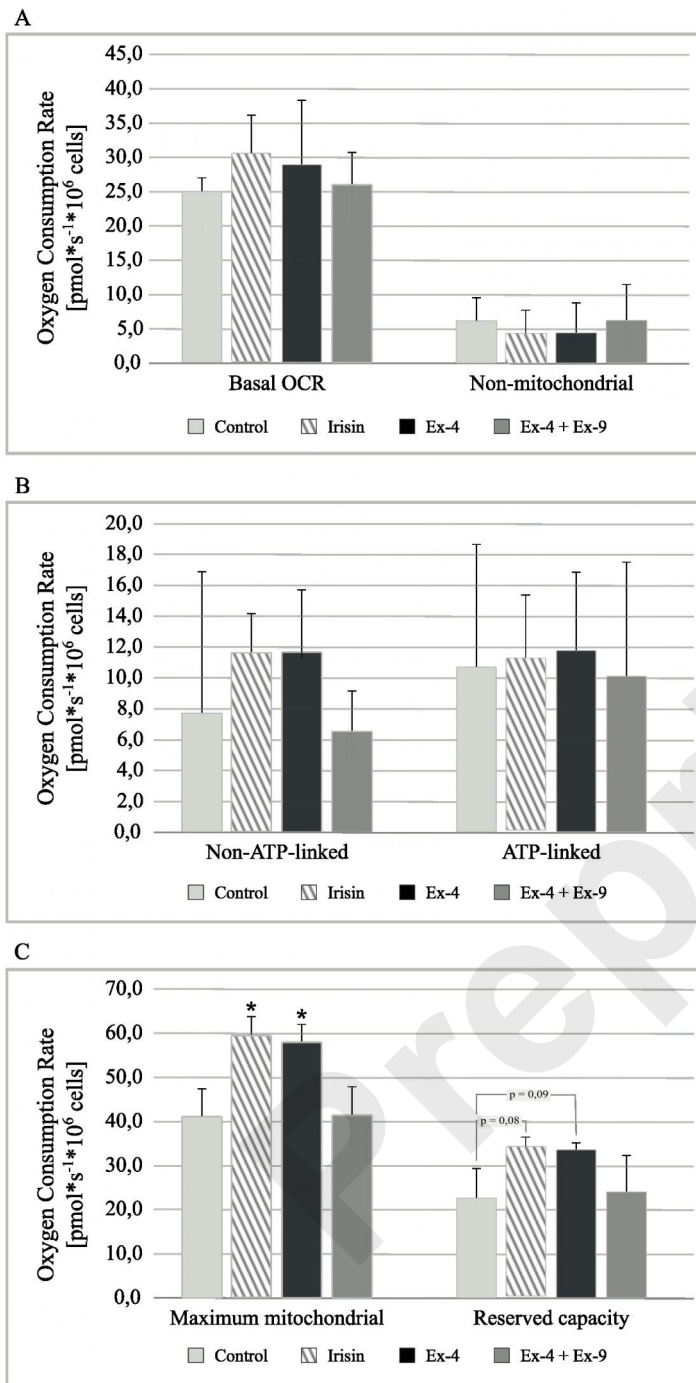


Figure 5. Oxygen consumption measured by high resolution respirometry (Oxygraph-2k, OROBOROS Instruments) in Chub-S7 control cells and cells incubated with irisin (250 ng/ml, 24 h), exendin-4 (Ex-4, 100 nM, 24h) or Ex-4 (100 nM, 24 h) +exendin-9 (Ex-4+Ex-9, 100 nM, 24 h). (A) basal oxygen consumption rate (OCR) and non-mitochondrial OCR. (B) Non-ATP and ATP-linked. (C) Maximum mitochondrial OCR and reserve capacity. Data presented as mean +S.D (n=3) analysed by T-test, \*p<0,05 compared to control.

### Intracellular ATP content

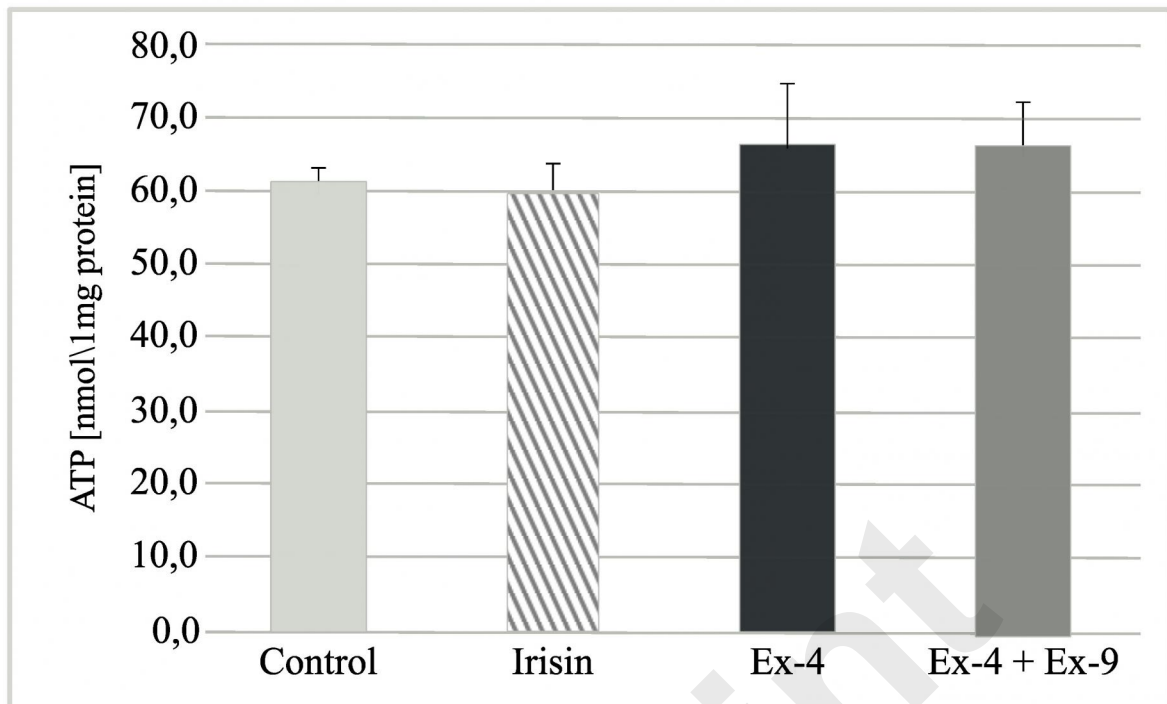


Figure 6. Intracellular ATP content in Chub-S7 control, irisin (250ng/ml, 24h) treated cells, exendin-4 (Ex-4, 100 nM, 24h) treated cells and exendin-4 (100 nM, 24h) +exendin-9 (Ex-4+Ex-9, 100 nM, 24h) treated cells. The results presented as nmol ATP/mg of cell protein, as mean +S.D. measured in triplicate, from 3 independent experiments. Analysed by T-test.